



PERGAMON

Available online at www.sciencedirect.com

SCIENCE @ DIRECT®

Solid-State Electronics 47 (2003) 2067–2074

SOLID-STATE
ELECTRONICS

www.elsevier.com/locate/sse

Exact analytical solution of channel surface potential as an explicit function of gate voltage in undoped-body MOSFETs using the Lambert W function and a threshold voltage definition therefrom

A. Ortiz-Conde ^{*}, F.J. García Sánchez, M. Guzmán

Laboratorio de Electrónica del Estado Sólido (LEES), Universidad Simón Bolívar, Apartado Postal 89000, Caracas 1080-A, Venezuela

Received 27 April 2003; accepted 15 May 2003

Abstract

Two useful applications of the Lambert W function to undoped-body MOSFET modeling are presented. Firstly, it is applied to the problem of inverting the gate voltage versus channel surface potential equation. The result is an exact analytical solution of the channel surface potential as an explicit function of the gate voltage for either n or p channel operation. Additionally an approximate but highly accurate analytical solution is presented which is continuously valid for all regions of operation. Secondly, we propose a new unambiguous analytical definition for the threshold voltage of these undoped-body devices. This definition overcomes the impossibility of using the traditional definition based on the bulk Fermi potential, and the ambiguities introduced by other definitions. The threshold voltage is mathematically described also using the Lambert W function at the transition point from subthreshold to superthreshold behavior. An approximation for the -1 branch of the Lambert W function is proposed to express the threshold voltage approximately using elementary logarithmic functions. These new descriptions are then verified against two-dimensional numerical device simulations.

© 2003 Elsevier Ltd. All rights reserved.

Keywords: Lambert function; Channel surface potential; MOSFET compact modeling; Intrinsic channel; Undoped-body; Threshold voltage

1. Introduction

The ongoing miniaturization of modern semiconductor devices is having considerable impact on their models parameters that are commonly associated with “bulk” properties. Among them, one of paramount importance in MOSFET modeling is impurity doping of the channel region. The inherent randomness of dopant impurity locations within a very short channel length,

not only turns questionable the concept of impurity density itself, but also gives rise in real life to significant fluctuations of the MOSFET characteristics. Of especial concern is the effect on the most important parameter, the threshold voltage [1]. To alleviate this serious problem, it has been proposed to do away with doping the channel region altogether and use instead an undoped (or lightly doped) body to sustain the channel. The idea, sometimes referred to as “intrinsic channel,” has been implemented in V-groove [2], double-gate SOI [3], and several kinds of epitaxial channel MOSFETs [4,5], and it is expected that it will become more prevalent in the future. In light of this possibility it seems pertinent to reconsider two fundamental concepts that are clearly affected by the absence of dopant atoms in

^{*} Corresponding author. Tel.: +58-212-9064010; fax: +58-290-63631.

E-mail addresses: ortizc@ieee.org (A. Ortiz-Conde), fgarcia@ieee.org (F.J. García Sánchez).

the channel region. They are the ability to express the channel surface potential as an explicit function of the terminal voltages, and the very meaning of the threshold voltage itself.

Accuracy and complexity of device models determine the effectiveness of simulation in IC design [6]. Compact MOSFET models of the “regional” type inherently incorporate continuity problems around the transition from the subthreshold region to the superthreshold region [7]. The accurate description of this transition becomes increasingly important considering the continuing dimensional downscaling and the reduction of the terminal voltages. Conversely, surface potential-based compact models are among the most accurate models available and have a higher content of physical meaning. They offer the advantage of being continuous portrayals valid throughout all regions of operation.

Surface potential-based models require that the channel surface potential be expressed in terms of the terminal voltages. Unfortunately, in the usual case of doped body devices, the surface potential is related to the gate voltage by a well known transcendental equation [6] that does not have a closed-form exact analytical solution. Therefore the surface potential is commonly obtained either by cumbersome numerical iteration, or by using some approximate solution [8,9]. In either case, a good initial guess for the surface potential is generally needed, or else the accuracy or computational efficiency can be seriously compromised [10], making such an otherwise desirable model unattractive from a practical point of view. However, for the particular case of undoped (or lightly doped) body, it is in fact possible to solve the surface potential as an explicit function of the terminal voltages. Such a solution will be derived, presented and verified in the next section.

Although the threshold voltage is the most important device parameter for the design, modeling, simulation and utilization of MOSFETs [6,7], its value is dependant upon its definition, which unfortunately is not always clearly stated when referring to this parameter. It is common in the literature to define a threshold voltage from a phenomenological point of view, as the gate voltage at which the surface potential at the Si–SiO₂ interface becomes approximately twice the bulk Fermi potential in the semiconductor body [6,7]. This definition is obviously unapplicable to undoped-body MOSFETs.

Attempts have been made to improve the threshold definition for doped devices [7,11]. For example, a new definition was proposed [12] to improve the accuracy of the V_T model for long-channel devices, but its improvement is less significant for MOSFETs with a channel length in the sub-micron range. A general graphical definition of threshold for uniformly doped body short-channel devices was proposed [13] as being the inter-

section of the two asymptotic equations of the surface potential versus gate voltage that dominate in the depletion and strong inversion regions. Other types of functional definitions exist for the threshold voltage [14], such as the de facto industry standard known as the “constant current definition,” based on the flow of a given pre-established level of drain current; or another closely related “critical current at threshold” that has been recently proposed for deep-submicron MOSFETs [15]. Considering the inadequacy of existing threshold voltage definitions for undoped-body long-channel devices, we propose in Section 3 a new unambiguous analytical definition for the threshold voltage of these devices, based on a mathematical description of the transition from the subthreshold region to the superthreshold region.

Second order considerations, such as Fermi–Dirac carrier distributions and quantum-mechanical effects [16], are neglected in the present study for the sake of simplicity. Their exclusion however should not affect the general validity of the conclusions, and it is possible to incorporate them without loss of generality for applications where they are significant.

2. Exact analytical expression for the surface potential

Charge-sheet analysis indicates that the relationship between the potential at the channel’s Si–SiO₂ interface of an enhancement MOSFET and the voltage at its gate, assuming zero drain-to-source and source-to-body voltages, can be expressed by the well known equation [6,7]:

$$(V_{GS} - V_{FB} - \psi_S)^2 = \frac{\epsilon_s^2}{C_{ox}^2} F^2(\psi_S), \quad (1)$$

where V_{GS} is the gate-to-source voltage, V_{FB} is the flat-band voltage, determined by the gate material-to-semiconductor body work function difference (neglecting interface trap and other oxide charges), ψ_S is the surface potential at the Si–SiO₂ interface, C_{ox} is the gate-oxide capacitance per unit area, ϵ_s is the permittivity of the semiconductor, and F is the Kingston function defined by [6]:

$$F^2(\psi_S) \equiv \frac{2qv_t}{\epsilon_s} \left\{ p_0 \left[\exp\left(-\frac{\psi_S}{v_t}\right) + \frac{\psi_S}{v_t} - 1 \right] + n_0 \left[\exp\left(\frac{\psi_S}{v_t}\right) - \frac{\psi_S}{v_t} - 1 \right] \right\}. \quad (2)$$

Here, $v_t = kT/q$ is the thermal voltage, and n_0 and p_0 are the equilibrium electron and hole concentrations. Since we are considering the case of channel enhancement in an undoped-body, the equilibrium electron and hole concentrations are equal to the intrinsic carrier density

n_i . Therefore, letting $n_0 = p_0 = n_i$, and substituting (2) into Eq. (1) yields

$$(V_{GS} - V_{FB} - \psi_S)^2 = \gamma^2 v_t \left[\exp\left(-\frac{\psi_S}{v_t}\right) + \exp\left(\frac{\psi_S}{v_t}\right) - 2 \right], \quad (3)$$

where

$$\gamma = \frac{\sqrt{2q\epsilon_s n_i}}{C_{ox}} \quad (4)$$

is the so-called body effect coefficient or body factor.

Taking the square root of Eq. (3) and expressing the exponential functions in terms of hyperbolic functions yields the equation that describes the gate voltage as a function of the channel surface potential for all regions of operation of an undoped-body device:

$$V_{GS} - V_{FB} - \psi_S = \text{sgn}(\psi_S) \gamma \sqrt{2v_t} \left[\cosh\left(\frac{\psi_S}{v_t}\right) - 1 \right]^{1/2}. \quad (5)$$

In this equation the $\text{sgn}(\psi_S)$ indicates that a minus sign is used when the bands bend up and a plus sign when the bands bend down. If we wish to circumvent the burden of changing signs during the calculation, we may use a half-angle trigonometric identity to get a more convenient equation continuously valid for any band bending:

$$V_{GS} - V_{FB} = \psi_S + 2\gamma\sqrt{v_t} \sinh\left(\frac{\psi_S}{2v_t}\right). \quad (6)$$

The above equation constitutes the complete description of gate voltage in terms of surface potential for the undoped-body device. Since we are generally interested in enhancing either an n-type or a p-type channel, we need only consider the corresponding positive or negative surface potentials. For example, for an n-type channel device, reverting (6) to exponential form yields:

$$V_{GS} - V_{FB} = \psi_S + \gamma\sqrt{v_t} \exp\left(\frac{\psi_S}{2v_t}\right), \quad (7)$$

where we have ignored the exponential with the negative exponent. We have further assumed that $\psi_S \gg v_t$, which allows to neglect the implicit “-1” term that should otherwise be added to the exponential to ensure that $V_{GS} - V_{FB}$ goes to zero as the surface potential approaches zero.

Since $n_0 \neq p_0 \neq n_i$ in the classical uniformly doped-body case, the linear surface potential terms in the RHS of (2) do not cancel each other. Their presence prevents obtaining an exact analytical solution of the surface potential in terms of the gate voltage. Fortunately this is not so when the body is undoped, since the absence of the linear surface potential terms in the Kingston function makes an analytical exact solution indeed possible

in this case. This possibility is highly desirable since precise description of at least up to the third order derivative with respect to the bias voltages is generally required for performing correct distortion analysis, among other reasons.

The exact solution that we propose makes use of the principal branch of the Lambert W function [17], a special function which cannot be expressed in terms of elementary functions, and is defined as the solution to the equation $W(x) \exp[W(x)] = x$. The Lambert W function has already proved its usefulness in numerous physics applications [18]. It has also been used for finding the solutions to several previously unsolved but basic diode [19] and bipolar transistor circuit analysis problems [20], and it can be found already incorporated into some circuit simulation tools.

The surface potential in (7) can be solved explicitly in terms of the Lambert W function to yield the following exact expression:

$$\psi_S = -2v_t W\left(\frac{\gamma}{2\sqrt{v_t}} \exp\left[\frac{(V_{GS} - V_{FB})}{2v_t}\right]\right) + V_{GS} - V_{FB}, \quad (8)$$

where W stands for the usual short-hand notation used for the principal branch of the “Lambert- W ” function.

Although (8) is indeed an exact solution of (7), strictly speaking the expression is not a physically “correct” solution of the surface potential, because of the simplifications that were made before attempting the solution. However, having neglected the -1 term introduces only a small error around the origin. If an accurate solution is in fact needed, it is easy to see that the inclusion of the “-1” term straightforwardly modifies the solution to

$$\psi_S = -2v_t W\left(\frac{\gamma}{2\sqrt{v_t}} \exp\left[\frac{(V_{GS} - V_{FB})}{2v_t} + \gamma\sqrt{v_t}\right]\right) + V_{GS} - V_{FB} + \gamma\sqrt{v_t}. \quad (9)$$

Evidently the additional terms in (9) are insignificant, except when $V_{GS} - V_{FB}$ approaches zero. It should be emphasized that (9) is the new exact analytical solution for the case of the n-type channel undoped-body device. Nonetheless, whenever we are not interested in exact values around the origin, it might be preferable not to include the additional terms and use (8) instead. Needless to say that this exact solution of the surface potential in the range of downward band-bending (n-type channel), has an analogous counterpart for upward band-bending (p-type channel).

Furthermore, if we need an expression for the surface potential continuously valid for all band-bending conditions (from n to p channel enhancement), (6) can be solved explicitly, also in terms of the Lambert W function, to yield an expression which in this case is only approximate:

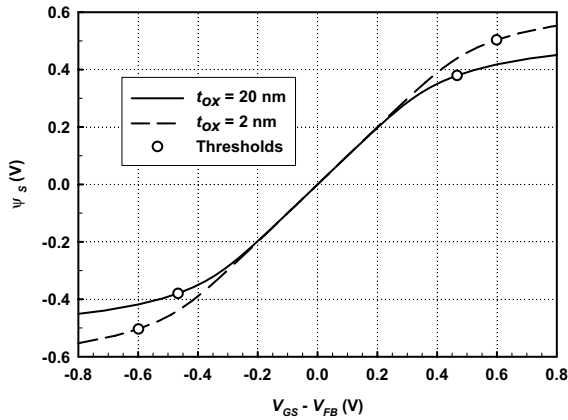


Fig. 1. Surface potential as a function of gate voltage calculated with (10) for an undoped-body long channel MOSFET, for two gate-oxide thicknesses, assuming zero drain-to-source voltage.

$$\psi_s = -2v_t W \left(\frac{\gamma}{2\sqrt{v_t}} \exp \left[\frac{(V_{GS} - V_{FB})}{2v_t} \right] \right) + 2v_t W \left(\frac{\gamma}{2\sqrt{v_t}} \exp \left[-\frac{(V_{GS} - V_{FB})}{2v_t} \right] \right) + V_{GS} - V_{FB}. \quad (10)$$

Fig. 1 presents the surface potential, ψ_s , versus gate voltage, V_{GS} , characteristics obtained using (10) for an undoped-body device, with gate-oxide thicknesses of 2 and 20 nm, assuming zero drain-to-source voltage.

The previous equation is an approximate analytical solution to Eq. (6), which represents a novel continuous representation of the surface potential in the full range of band-bending, for the particular case of an undoped (or lightly doped) body. Although strictly speaking (10) is not mathematically exact, it is nonetheless extremely accurate for the typical range of parameter values characteristic to the present type of problems. Fig. 2 shows the absolute error as a function of gate voltage, resulting from calculating the surface potential with (10). As shown, for an oxide thickness of 20 nm, the maximum error incurred by calculating the surface potential with (10) is about 8 nV, and occurs in this case around a $V_{GS} - V_{FB}$ of 0.4 V. This maximum error decreases for diminishing oxide thickness to values as low as 80 pV for an oxide thickness of 2 nm, also shifting its location to higher gate voltages around $V_{GS} - V_{FB} = 0.5$ V.

The above results were verified against two-dimensional (2-D) numerical device simulations. Fig. 3 presents with symbols the resulting values of the surface potential calculated at the middle of the channel for several gate voltages, of a long-channel undoped-body MOSFET with a 20 nm thick gate-oxide and a flat-band

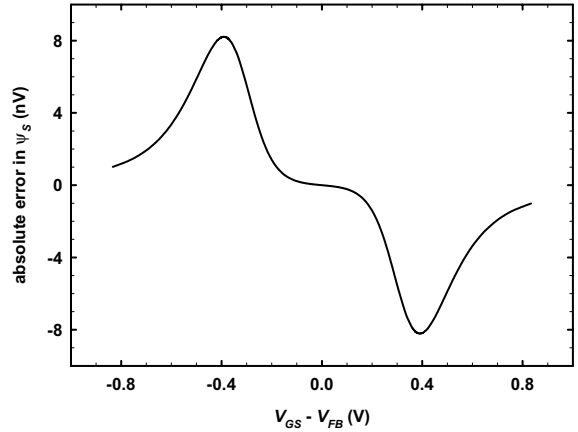


Fig. 2. Absolute error as a function of the gate voltage resulting from calculating the surface potential with (10) for a gate-oxide thickness of 20 nm.

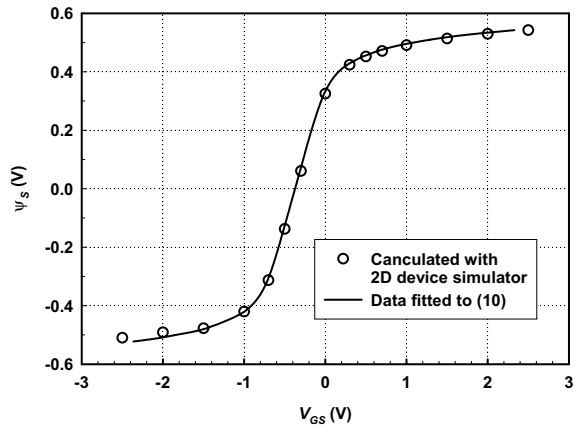


Fig. 3. Middle of the channel surface potential at several values of gate voltage (symbols), of a long-channel undoped-body MOSFET with a 20 nm gate-oxide thickness, as calculated with a 2-D device simulator, and the corresponding function (line) obtained by fitting these points to (10).

voltage of -0.372 V. The continuous line in the graph shows the result of fitting those points to (10). The 2-D simulated surface potential values compare very well to the analytically calculated ones. This same 2-D device simulation will be used again latter for comparison purposes by extracting its threshold voltage from its drain current characteristics.

3. Defining the threshold voltage of undoped-body devices

In the increasingly important case of MOSFETs with undoped channel regions, it is obvious that the traditional and widely accepted definition of threshold volt-

age, based on the bulk Fermi potential, becomes meaningless [21]. It has been suggested [8] that the threshold voltage of these devices should be defined as the gate voltage that produces a certain pre-established constant value of mobile charge in the channel. Although this is an undoubtedly simple definition, it clearly depends on an arbitrary choice of a predetermined value of charge, in a similar way as does the traditional industry standard constant-current threshold voltage definition. Considering the inherent ambiguity that this type of definitions introduces, we propose here a new unambiguous analytical definition for the threshold voltage of undoped-body long-channel devices. It follows from a previously proposed graphical definition of the threshold voltage of doped body devices [13]. The novel definition is based on the mathematical description underlying the concept of the transition from the subthreshold region to the superthreshold region. It takes into consideration the asymptotic behavior of the two surface potential functions that describe each of these subthreshold and superthreshold regions. In spite of the undoped-body, we will still refer to these two regions as the weak and strong “inversion” regions of operation, to maintain the analogy to classical doped-body devices.

Recalling (7) for the n-channel device and considering the corresponding dominant terms for each bias condition, we can obtain the following two asymptotic equations at the two distinct regions of operation:

$$V_{GS} - V_{FB} \approx \gamma\sqrt{v_t} \exp\left(\frac{\psi_S}{2v_t}\right), \quad (11)$$

for the superthreshold (strong inversion) region, and

$$V_{GS} - V_{FB} \approx \psi_S, \quad (12)$$

for the subthreshold (weak inversion) region. The same argument about the absence of the “-1” term in (7) could also be made in (11), but in this case it would really be pointless to include it, since we are interested in the threshold voltage and not in values near the origin.

What we propose is that the onset of strong inversion, the “threshold,” lies at the transition point where strong inversion behavior, as described by asymptotic equation (11), begins to dominate over weak inversion behavior, as described by asymptotic equation (12). In other words, it is the point at which the surface potential behavior changes from predominantly linear-like to predominantly logarithmic-like, with respect to the applied gate voltage. Accordingly, the point where the two asymptotic equations (11) and (12) intersect is said to give the value of the threshold voltage, V_T . This point is not only mathematically convenient but it is also physically meaningful for defining the threshold voltage of the undoped-body MOSFET, as will be shown below.

The new analytical definition for the threshold voltage (henceforth referred to as “the asymptotic V_T ”) of undoped-body long-channel MOSFETs is obtained readily by solving Eqs. (11) and (12):

$$V_T = V_{FB} - 2v_t W_- \left(-\frac{\gamma}{2\sqrt{v_t}} \right), \quad (13)$$

where the symbol W_- represents the -1 branch of the Lambert W function. It might be noted for completeness sake, that the other solution, corresponding to the principal branch of the Lambert W function, given by

$$V_T = V_{FB} - 2v_t W \left(-\frac{\gamma}{2\sqrt{v_t}} \right), \quad (14)$$

must be discarded because it is physically unreasonable.

The corresponding value of surface potential at threshold may be found if needed by substituting (13) into (8). Fig. 4 illustrates the surface potential, ψ_S , versus positive gate voltage, V_{GS} , as obtained with (8) or (9) for a gate-oxide thickness of 20 nm. Also presented are the two superthreshold and subthreshold asymptotic equations of ψ_S , (11) and (12), corresponding to the strong and weak inversion regions. The projection of the intersection to the V_{GS} -axis graphically describes the threshold voltage of the device as defined by (13).

Although (13) is a sufficiently simple expression, it might be desirable for quick hand calculations to be able to use an approximate expression in terms of elementary analytical functions. Several approximations have been proposed for the branches of the Lambert W function [18,20]. We propose to use the following convenient approximation for the negative branch of the Lambert

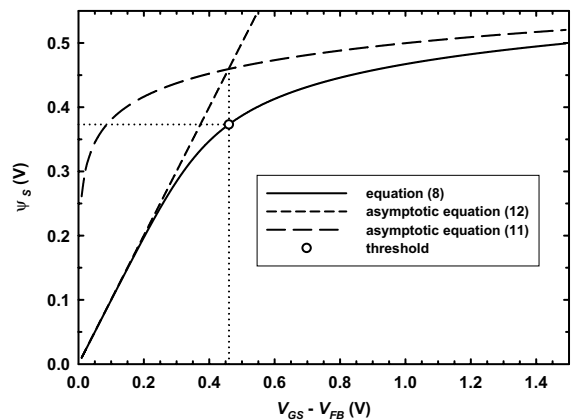


Fig. 4. Surface potential versus positive gate voltage, V_{GS} , as obtained with Eq. (8) for a gate-oxide thickness of 20 nm. Also presented are the two superthreshold and subthreshold asymptotic behaviors, (11) and (12). The projection of the intersection to the horizontal axis graphically defines the “asymptotic threshold voltage” with a value of 0.467 V for this device.

W function valid at very small negative values of the argument:

$$W_-(x) \approx \ln \left[\frac{x}{\ln(-x)} \right]. \quad (15)$$

Replacing (15) for the negative branch of the Lambert W function in (13) we obtain an approximate logarithmic expression for the threshold voltage:

$$V_T = V_{FB} - 2v_t \ln \left[\frac{-\frac{\gamma}{2\sqrt{v_t}}}{\ln \left(\frac{\gamma}{2\sqrt{v_t}} \right)} \right]. \quad (16)$$

Since there is no fixed charge in the undoped semiconductor body, the total charge in the semiconductor, Q_S , is the carrier charge per unit area induced in the channel, which can be calculated from (10):

$$\begin{aligned} Q_S &\equiv V_{ox}C_{ox} = (\psi_S - V_{GS} + V_{FB})C_{ox} \\ &= -2v_tC_{ox}W \left(\frac{\gamma}{2\sqrt{v_t}} \exp \left[\frac{(V_{GS} - V_{FB})}{2v_t} \right] \right) \\ &\quad + 2v_tC_{ox}W \left(\frac{\gamma}{2\sqrt{v_t}} \exp \left[-\frac{(V_{GS} - V_{FB})}{2v_t} \right] \right). \end{aligned} \quad (17)$$

Fig. 5 presents the carrier charge per unit area in the channel versus the applied gate voltage, as calculated with (17), for two values of gate-oxide thickness, assuming zero flat-band voltage and zero drain-to-source voltage. Also shown in the figure are the linear extrapolations to zero charge, which represent the basic conceptual principle of threshold voltage. The values shown of ± 0.599 and ± 0.467 V, for oxide thickness of 2 and 20 nm, respectively, match closely the corresponding

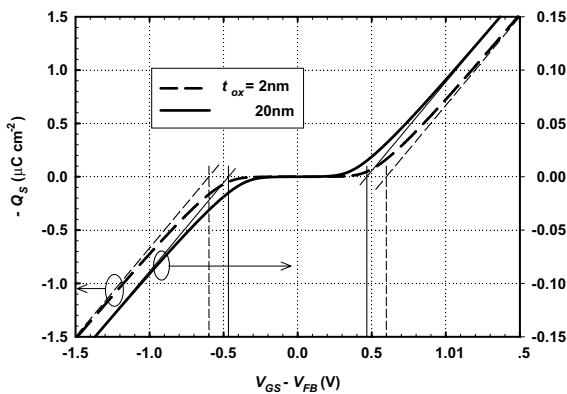


Fig. 5. Semiconductor (carrier) charge per unit area in the channel as a function of applied gate voltage, for two values of gate-oxide thickness, assuming zero drain-to-source voltage, as calculated by (17). Also shown are the linear extrapolations and their intersections with the voltage axis that indicate the values of the positive and negative threshold voltages of ± 0.599 and ± 0.467 V.

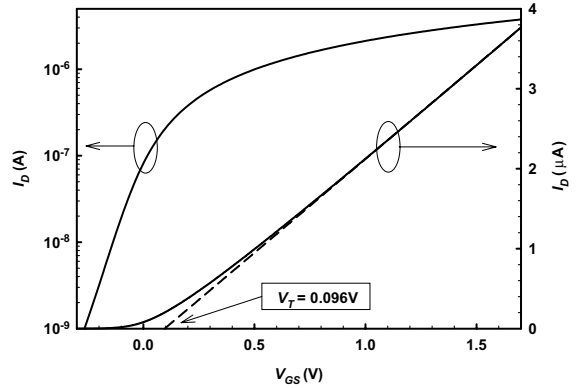


Fig. 6. Extraction of the threshold voltage from the linear extrapolation of the drain current as a function of gate voltage of a long channel undoped-body MOSFET with a 20 nm thick gate-oxide and $V_{FB} = -0.372$ V, calculated using a 2-D device simulator. The extracted value matches that obtained from (13) when the flat-band voltage of -0.372 V is added.

threshold voltages calculated with (13). This carrier charge per unit area in the channel as calculated with (17) agree very well with the values obtained from 2-D device simulations of the long channel undoped-body MOSFET.

In order to compare the values of threshold voltage indicated by the proposed “asymptotic definition” to actual values extracted from transfer characteristics, we used the 2-D device simulator, to calculate the drain current of the long channel undoped-body MOSFET with a 20 nm thick gate-oxide and a flat-band voltage of -0.372 V. Fig. 6 presents the drain current as a function of gate voltage. From this transfer characteristic we may extract the threshold voltage of the device using the common extraction method of linear extrapolation [14]. When the flat-band voltage $V_{FB} = -0.372$ V used in the simulation is subtracted from the extracted value of $V_T = 0.096$ V, the resulting value of $V_T - V_{FB} = 0.468$ V matches very well the value of 0.467 V calculated from (13) for this 20 nm thick gate-oxide device.

4. Discussion

The value of threshold voltage indicated by this asymptotic definition, whether obtained graphically or calculated with (13), is the same that results from linearly extrapolating the semiconductor charge to zero (Fig. 5), and also matches closely the value actually extracted from the linear extrapolation of the drain current transfer characteristics, generated from 2-D device simulation (Fig. 6). The corresponding value of the surface potential at threshold can be found by substituting the calculated V_T into (8).

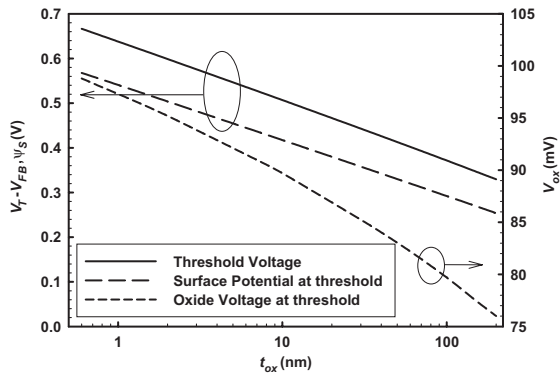


Fig. 7. Variation of threshold voltage, surface potential at threshold, and the corresponding oxide voltage dependence on gate-oxide thickness.

It should be remembered that, for simplicity's sake, the original formulation is based on Maxwell–Boltzmann, not on Fermi–Dirac, occupation probability distribution statistics. Thus, the calculated surface potential values, and the corresponding carrier charge-sheet density, near $E_g/2q$ are not exactly accurate; but this consideration should not greatly affect the validity of the present results for gate-oxide thicknesses > 2 nm.

The curves of Figs. 1, 3 and 5 evidence the symmetric nature of the channel enhancement mechanism (n or p) of these undoped-body devices. The expected linear increase of the carrier charge-sheet density with gate voltage is clearly seen in Fig. 5, at values well above the threshold voltage. This behavior is then reflected upon the drain current as observed in Fig. 6.

The dependence of the threshold voltage on gate-oxide thickness, as calculated using (13) is presented in Fig. 7. The resulting plot confirms that the threshold voltage of undoped-body devices, as described by this new asymptotic- V_T definition, decreases essentially as a linear function of the logarithm of oxide thickness. This behavior, although atypical in highly doped-body devices, is what should be expected for undoped-bodies. We have also confirmed that it occurs even for lightly doped bodies, when doping concentrations are less than about 10^{15} cm $^{-3}$, above which level the conventional behavior is again exhibited.

5. Conclusions

Design and modeling of undoped-body MOSFETs would benefit from computationally efficient and physically meaningful surface-potential compact models. To that end we have developed, using Lambert W functions, an exact analytical solution of the surface potential as an explicit function of the gate voltage, valid for either

upward or downward band-bending. Additionally we have also presented a highly accurate analytical solution which is continuously valid for all regions of operation of this particular kind of device.

Modeling undoped-body MOSFETs also requires a more unambiguous definition of threshold voltage than what is presently provided by conventional definitions. To that end, we have proposed a new approach for defining V_T based on finding the intersection of the surface potential versus gate voltage asymptotic equations for the so-called weak and strong inversion regions. The resulting new definition is also expressed in terms of the Lambert W function.

It has been shown that this threshold voltage, as defined by such intersection, matches the value of V_T determined by extrapolating the carrier charge-sheet density to zero. We have also obtained very good agreement between the 2-D device simulation and both, our analytical solution, and the threshold voltage definition model. It is our conviction that the proposed asymptotic definition of V_T promises to be a dependable means to unambiguously define the threshold voltage of future undoped-body MOSFET devices. Additionally, we expect that the exact explicit solution that has been presented here could become a useful foundation for the formulation of future surface potential-based compact models for this kind of undoped-body MOSFETs.

References

- [1] Takeuchi K, Koh R, Mogami T. A study of the threshold voltage variation for ultra-small bulk and SOI CMOS. *IEEE Trans Electron Dev* 2001;ED-48:1995–2001.
- [2] Appenzeller J, Martel R, Avouris Ph, Knoch J, Scholvin J, del Alamo JA, et al. Sub-40 nm SOI V-groove n-MOSFETs. *IEEE Electron Dev Lett* 2002;EDL-23:100–2.
- [3] Taur Y. An analytical solution to a double-gate MOSFET with undoped body. *IEEE Electron Dev Lett* 2000;EDL-21:245–7.
- [4] Wong HS, Chan KK, Lee Y, Roper P, Taur Y. Fabrication of ultrathin, highly uniform thin-film SOI MOSFETs with low series resistance using pattern-constrained epitaxy. *IEEE Trans Electron Dev* 1997;EDL-44:1131–5.
- [5] Ohguro T, Naruse H, Sugaya H, Morifuji E, Nakamura S, Yoshitomi T, et al. An 0.18- μ m CMOS for mixed digital and analog applications with zero-volt- V_{th} epitaxial-channel MOSFETs. *IEEE Trans Electron Dev* 1999;ED-46:1378–83.
- [6] Liou JJ, Ortiz-Conde A, García Sánchez FJ. Design and analysis of MOSFETs: modeling, simulation and parameter extraction. Boston: Kluwer Academic Publisher; 1998.
- [7] Tsividis YP. Operation and modeling of the MOS transistor. New York: McGraw Hill; 1987.
- [8] Chen TL, Gildenblat G. Analytical approximation for the MOSFET surface potential. *Solid-State Electron* 2001;45:335–9.

- [9] Shigyo N. An explicit expression for surface potential at high-end of moderate inversion. *IEEE Trans Electron Dev* 2002;ED-49:1265–73.
- [10] McAndrew CC, Victory JJ. Accuracy of approximations in MOSFET charge models. *IEEE Trans Electron Dev* 2002;ED-49:72–81.
- [11] Benson J, D'Halleweyn NV, Redman-White W, Easson CA, Uren MJ, Faynot O, et al. A physically based relation between extracted threshold voltage and surface potential flat-band voltage for MOSFET compact modeling. *IEEE Trans Electron Dev* 2001;48:1019–21.
- [12] Ortiz-Conde A, Rodríguez J, García Sánchez FJ, Liou JJ. An improved definition for modeling the threshold voltage of MOSFETs. *Solid-State Electron* 1998;42:1743–6.
- [13] Salcedo JA, Ortiz-Conde A, García Sanchez FJ, Muci J, Liou JJ, Yue Y. New approach for defining the threshold voltage of MOSFETs. *IEEE Trans Electron Dev* 2001;ED-48:809–13.
- [14] Ortiz-Conde A, García Sánchez FJ, Liou JJ, Cerdeira A, Estrada M, Yue Y. A review of recent MOSFET threshold voltage extraction methods. *Microelectron Reliab* 2002;42:583–96.
- [15] Zhou X, Lim KY, Qian W. Threshold voltage definition and extraction for deep-submicron MOSFETs. *Solid-State Electron* 2001;45:507–10.
- [16] Gildenblat G, Chen TL, Bendix P. Closed-form approximation for the perturbation of MOSFET surface potential by quantum-mechanical effects. *Electron Lett* 2000;36:1072–3.
- [17] Corless RM, Gonnet GH, Hare DEG, Jeffrey DJ, Knuth DE. On Lambert's W function. *Adv Comput Math* 1996;5:329–59.
- [18] Valluri SR, Jeffrey DJ, Corless RM. Some applications of the Lambert W function to physics. *Can J Phys* 2000;78:823–31.
- [19] Ortiz-Conde A, García Sánchez FJ, Muci J. Exact analytical solutions of the forward non-ideal diode equation with series and shunt parasitic resistances. *Solid-State Electron* 2000;44:1861–4.
- [20] Banwell TC. Bipolar transistor circuit analysis using the Lambert W -function. *IEEE Trans Circ Syst I* 2000;47:1621–33.
- [21] Chen Q, Bowman KA, Harrell EM, Meindl JD. Double jeopardy in the nanoscale court. *IEEE Circ Dev Mag* 2003;19:28–34.